ACS Catalysis

Research Article

pubs.acs.org/acscatalysis

Stereoselective Oxidation of Aryl-Substituted Vicinal Diols into Chiral α-Hydroxy Aldehydes by Re-Engineered Propanediol Oxidoreductase

Cecilia Blikstad,[†] Käthe M. Dahlström,[‡] Tiina A. Salminen,[‡] and Mikael Widersten*[,†]

[†]Department of Chemistry−BMC, Uppsala University, Box 576, SE-751 23 Uppsala, Sweden

[‡]Structural Bioinformatics Laboratory, Åbo Akademi University, Tykistökatu 6A, FIN-20520 Turku, Finland

Supporting Information

ABSTRACT: α-Hydroxy aldehydes are chiral building blocks used in synthesis of natural products and synthetic drugs. One route to their production is by regioselective oxidation of vicinal diols and, in this work, we aimed to perform the oxidation of 3-phenyl-1,2-propanediol into the corresponding α-hydroxy aldehyde applying enzyme catalysis. Propanediol oxidoreductase from *Escherichia coli* efficiently catalyzes the stereoselective oxidation of *S*-1,2-propanediol into *S*-lactaldehyde. The enzyme, however, shows no detectable activity with aryl-substituted or other bulky alcohols. We conducted ISM-driven directed evolution on FucO and were able to isolate several mutants that were active with *S*-3-phenyl-1,2-propanediol. The most efficient variant displayed a k_{cat}/K_M of 40 s^{-1} M^{-1} and the most enantioselective variant an E-value (*S*/*R*) of 80. Furthermore, other isolated variants showed up to 4400-fold increased activity with another bulky substrate, phenylacetaldehyde. The results with engineered propanediol oxidoreductases identified amino acids important for substrate selectivity and asymmetric synthesis of aryl-substituted α-hydroxy aldehydes. In conclusion, our study demonstrates the feasibility of tailoring the catalytic properties of propanediol oxidoreductase for biocatalytic properties.

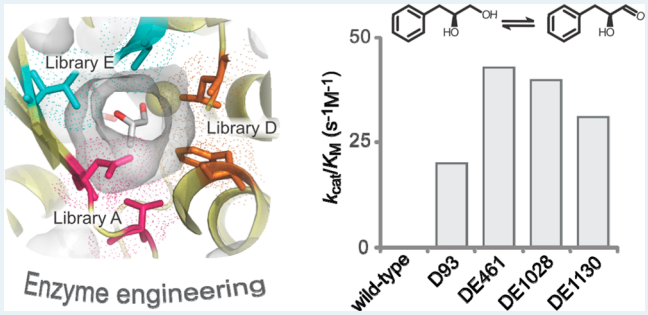

KEYWORDS: *biocatalytic diol oxidation, regioselectivity, directed enzyme evolution, principal components analysis, steady-state kinetics*

INTRODUCTION

The carbonyl group is arguably the most important functional group in biomolecules. Proteins, carbohydrates, nucleic acids, lipids, various metabolites, and a number of cofactors all contain carbonyl groups in various forms: esters, carboxylic acids, ketones, amides, and aldehydes. The polar character and hydrogen bonding capacity of the carbonyl group stabilize biomolecular structures and enable intra- and intermolecular interactions necessary in essential life processes such as storage and transfer of genetic information, chemical catalysis by enzymes, and ion transport. The reactivities and physicochemical properties of carbonyl containing molecules place them as essential building blocks in metabolic reactions involving aldol condensations, redox reactions, racemizations, sugar cyclizations, amino- and acyl transfer, amidations, and isomerizations. The same reaction types are equally important in synthetic chemistry, in design and production of pharmaceutical drugs, where carbonyls are utilized for interaction with target biomolecules or as attachment points for addition of other functional groups and site-specific derivatizations.

α-Hydroxy-substituted aldehydes and ketones are found naturally in aldose and ketose sugars and are important chiral building blocks in the synthesis of natural products and synthetic drugs.[1−4] Their synthesis is, however, not trivial because of their intrinsic reactivity and thereby tendency to participate in unwanted side reactions (e.g., ref 5). In cells, ketones and aldehydes can be formed from oxidation of secondary or primary alcohols, respectively. These transformations are typically catalyzed by dehydrogenases utilizing nicotinamide cofactors ($NAD(P)^+$) as electron acceptors. As these enzymes are generally unprecedented in their catalytic powers and stereoselectivity, attempts to harness their efficiencies for synthetic purposes have been conducted.[6−9] A limiting factor for the use of biocatalysis is the limited substrate scope of most naturally occurring enzymes. This limitation can now, however, be addressed in favorable cases using current methodology for re-engineering of enzyme structures to improve their suitability as biocatalysts.[10]

Propanediol oxidoreductase from *Escherichia coli*, FucO (EC:1.1.1.77), participates in the catabolism of unusual carbohydrates such as fucose and rhamnose.[11] FucO catalyzes the reversible conversion of the three-carbon α-hydroxy aldehyde *S*-lactaldehyde and *S*-1,2-propanediol utilizing $NADH/NAD^+$ as cofactors (Scheme 1A). The strict

Received: July 8, 2013
Revised: November 1, 2013
Published: November 4, 2013

Scheme 1. (A) Interconversion of *S*-2-Hydroxypropanal (*S*-lactaldehyde) and *S*-1,2-Propanediol Catalyzed by FucO Using NAD(H) as a Cofactor; (B) Serial Epoxide Hydrolysis and Primary Alcohol Oxidation Producing a α-Hydroxyl Substituted Aldehyde[a]

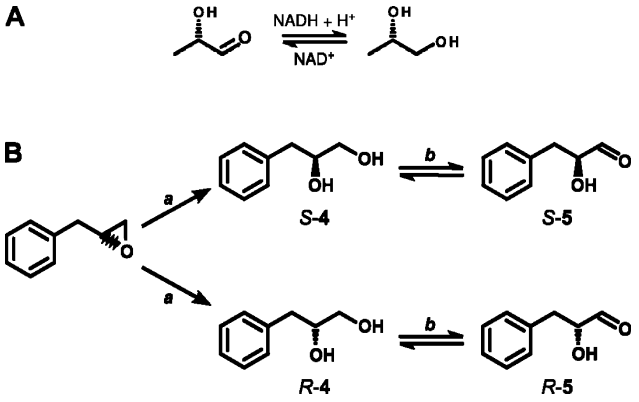

[a] *a*, Hydrolysis of *S*- or *R*-(2,3-epoxypropyl)benzene by epoxide hydrolase; *b*, oxidation of *S*- or *R*-**4** into the corresponding α-hydroxy aldehydes (*S*- or *R*-**5**) by FucO variant and NAD^+.

regioselectivity displayed by the FucO enzyme in the oxidation of vicinal diols is attractive from the prospect of possible biocatalytic production of chiral α-hydroxy aldehydes by the use of this enzyme. FucO, however, because of its biological role, is not active with larger phenyl-substituted alcohols,[12] which restricts its biocatalytic potential. Our intent for FucO was to catalyze regio- and enantioselective oxidation of aryl-substituted vicinal diols such as phenylpropanediols, *R*- and *S*-**4** (Chart 1). These diols are products of epoxide hydrolase catalyzed hydrolysis of (2,3-epoxypropyl)benzene,[13,14] and one aim was to produce, by protein engineering, FucO variants capable of catalyzing the oxidation of diol **4** and thereby enable a two-step transformation of (2,3-epoxypropyl)benzene into the α-hydroxy aldehyde products **5** (Scheme 1B).

Chart 1. Compounds Applied as Substrates for FucO Variants: 1-Propanol (1), *S*-1,2-Propanediol (*S*-2), *R*-1,2-Propanediol (*R*-2), Phenylacetaldehyde (3), *S*-3-Phenyl-1,2-propanediol (*S*-4), and *R*-3-Phenyl-1,2-propanediol (*R*-4)

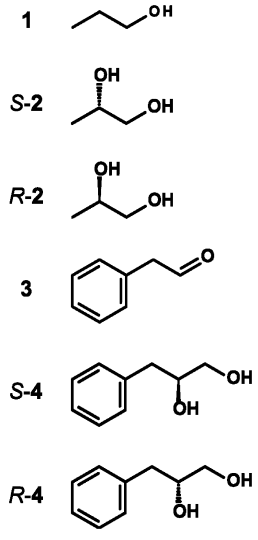

FucO is a homodimeric protein with a classical Rossman folded coenzyme binding site[15] (Figure 1A). The enzyme

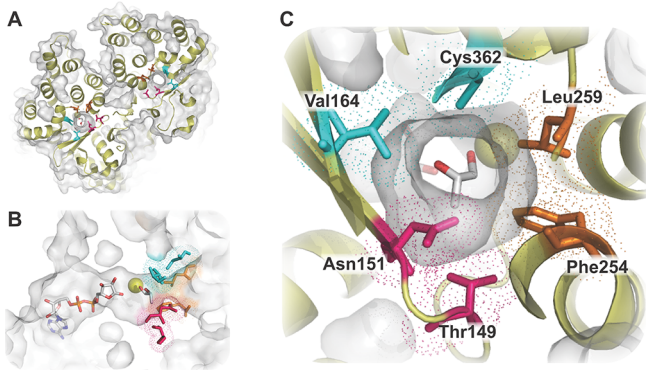

Figure 1. (A) Dimeric structure of FucO. (B) The binding sites for the cofactor and the alcohol/aldehyde. (C) The alcohol/aldehyde binding site. The view is rotated 90 degrees around the *y*-axis from the view in (B) to show the active site from the entry point of the alcohol/aldehyde substrate. Residues mutated to create libraries of variant FucO enzyme are indicated by stick models. Library A: T149, N151 (magenta); library C: V164 (cyan); library D: F254 and L259 (orange), and library E: V164 and C362 (cyan). NAD(H) analogue adenosine-5-diphosphoribose (gray) and *S*-1,2-propanediol (gray) are presented as stick models, active-site iron(II) is shown as a sphere (yellow), and the polypeptide chain as surface and cartoon. The image was created in PyMOL (ver. 1.5 www.pymol.org) from the atomic coordinates in 1RRM.[15]

belongs to the class III alcohol dehydrogenases, which are considered to be Fe(II) dependent.[16] The entrance for the substrate into the active site is narrow and limits the size of allowed substrates (Figure 1B). Hence, the protein structure requires remodeling to oxidize bulky substrates such as diol **4**. FucO was therefore subjected to directed evolution to produce variant enzymes. Mutagenesis was guided by inspection of available crystal structures,[15] and the targeted amino acid residues were considered to restrict entry to the active site (Figure 1C). Mutations were introduced according to the iterative saturation mutagenesis (ISM) approach as described by Reetz and co-workers.[17,18] By coupling the ISM-driven mutagenesis with direct assays of enzyme activities in the generated mutants, we have isolated variant FucO enzymes capable of catalyzing redox transformations on aryl-substituted substrates.

EXPERIMENTAL SECTION

Chemical and Reagents. Commercially available chemicals were purchased from Sigma-Aldrich at the highest purity available. Chiral purity of *S*- or *R*-1,2-propanediol were ≥96%. *S*- or *R*-(2,3-epoxypropyl)benzene at >98% chiral purity were purchased from TCI Europe N.V. Oligonucleotides used in mutagenesis and library constructions were custom-ordered from Thermo Scientific. Enzymes and reagents for molecular biology work were purchased from Fermentas. Chromatographic resins were purchased from GE Healthcare. The *S*- and *R*-enantiomers of **4** were synthesized by *Solanum tuberosum* epoxide hydrolase (StEH1) catalyzed ring-opening of the corresponding epoxide enantiomers; 50 or 100 mM of *S*- or *R*-(2,3-epoxypropyl)benzene, 1.5−3 μM of StEH1, and 3.3 mM acetonitrile was added to 100 or 10 mM sodium-phosphate, pH 7.0, respectively.[13] Reactions were carried out overnight at

dx.doi.org/10.1021/cs400824h | *ACS Catal.* 2013, 3, 3016−3025

room temperature under mild shaking (~20 rpm) in 15 mL reaction volumes contained in 50 mL Erlenmeyer glass flasks. The StEH1-catalyzed epoxide hydrolysis retains the configurations of the corresponding epoxides.[14]

Library Design. On the basis of previous functional analyses[12] and investigation of crystal structures of FucO,[15] six amino acid residues were targeted for mutagenesis with the anticipated effect of altering substrate selectivity. These residues line the entrance of the substrate binding site. The six residues were divided into four different focused libraries: Library A, Thr149 and Asn151; Library C, Val164; Library D, Phe254 and Leu259; and Library E, Val164 and Cys362. For construction of the second-generation library AD FucO variant A5 (N151G) was used as template gene and for library DA and DE variant D93 (L259V) were used. For third-generation library DAE the DE1472 (N151G, L259V) was used as template. A combination of saturation mutagenesis and limited codon sets were used (Table 1).[19]

Library Constructions. In the construction of first-generation libraries, plasmid pGTacfucO-5H encoding wild-type FucO[12] was used as template. Sequences of mutagenic oligonucleotides and the codon replacements are shown in Supporting Information, Table SI1. Mutated PCR fragments were subcloned between the *Xho*I and *Spe*I restriction sites of pGTacStEH1-5H.[20] The resulting expression plasmids were transformed into *E. coli* XL1-Blue by electroporation. A pool of 500−1000 clones from each library were sequenced to confirm expected mutations and to assess library quality based on introduced codon/mutation distribution.[21]

Small-Scale Protein Expression and Lysate Preparation for Activity Screening. Expression of library enzymes was carried out in 96-well plates. The procedure was essentially according to a previously described protocol used for protein expression in library screening of StEH1 mutants,[13] with the exception that after bacteria inoculation the cultures were grown for 3.5 h and at the time of induction of transcription, 100 μM $FeCl_2$ was added together with the IPTG inducer. The microtiter plates were inoculated with library clones together with four clones of each control; wild-type FucO and StEH1 (as internal negative controls) and four wells were left without inoculate. For the second- and third-generation libraries, the parent variants (A5, D93, and DE1472) were also included as controls. The initial protocol as described by Gurell and Widersten[13] was followed up to the point of bacteria harvest. After removal of the supernatant bacterial pellets were prepared for screening. Twenty-five microliters of B-PER (Pierce) fortified with 0.2 mg/mL DNase I, 0.2 mg/mL lysozyme and protease inhibitor (Complete Protease Inhibitor Cocktail Tablets EDTA-free from Roche) were added to each well. The pellets were resuspended by mild vortexing, and the mixtures were incubated at mild shaking at room temperature for 1 h. Subsequently, 100 μL of 10 mM sodium-phosphate buffer, pH 7.0, was added to each well, and the plates were centrifuged at 3,500 *g* for 60 min, at 4 °C.

Library Screening. After cell lysis and centrifugation 20 μL of lysate from each well were transferred to a polystyrene 96-well microtiter plate with flat bottom (Nunc). Buffer, cofactor and substrate were mixed together and preincubated at 30 °C. The reaction mixtures were thereafter added to the lysate-containing microtiter plate to a final volume of 150 μL and enzyme activity was measured for 3 to 5 min. Reaction velocities were monitored spectrophotometrically at 30 °C through the change in NADH concentration at 340 nm ($\Delta\varepsilon$ =

Table 1. Codon Subsets in Gene Libraries for Variant FucO Enzymes

	position								
library	149[a]	151[a]	164[a]	254[a]	259[a]	362[a]	codon set	theoretical number of protein variants	screened number of clones
A	DCC *A, S, T*	NNS *all 20*					96	60	304
C			NNS *all 20*				32	20	156
D				KYC *A, F, S, V*	KYA *A, L, S, V*		16	16	156
AD		N151G		NDT *C, D, F, G, H, I, L, N, R, S, V, Y*	NDT *C, D, F, G, H, I, L, N, R, S, V, Y*		144	144	608
DA	NNS *all 20*	NDT *C, D, F, G, H, I, L, N, R, S, V, Y*			L259V		384	240	1216
DE			NDT, VMA, ATG, TGG *all 20*		L259V	NDT, VMA, ATG, TGG *all 20*	400	400	1152
DAE		N151G	NDT, VMA, ATG, TGG *all 20*		L259V	NDT, VMA, ATG, TGG *all 20*	400	400	1152

[a]Codon set *encoded amino acid.*

dx.doi.org/10.1021/cs400824h | *ACS Catal.* 2013, 3, 3016−3025

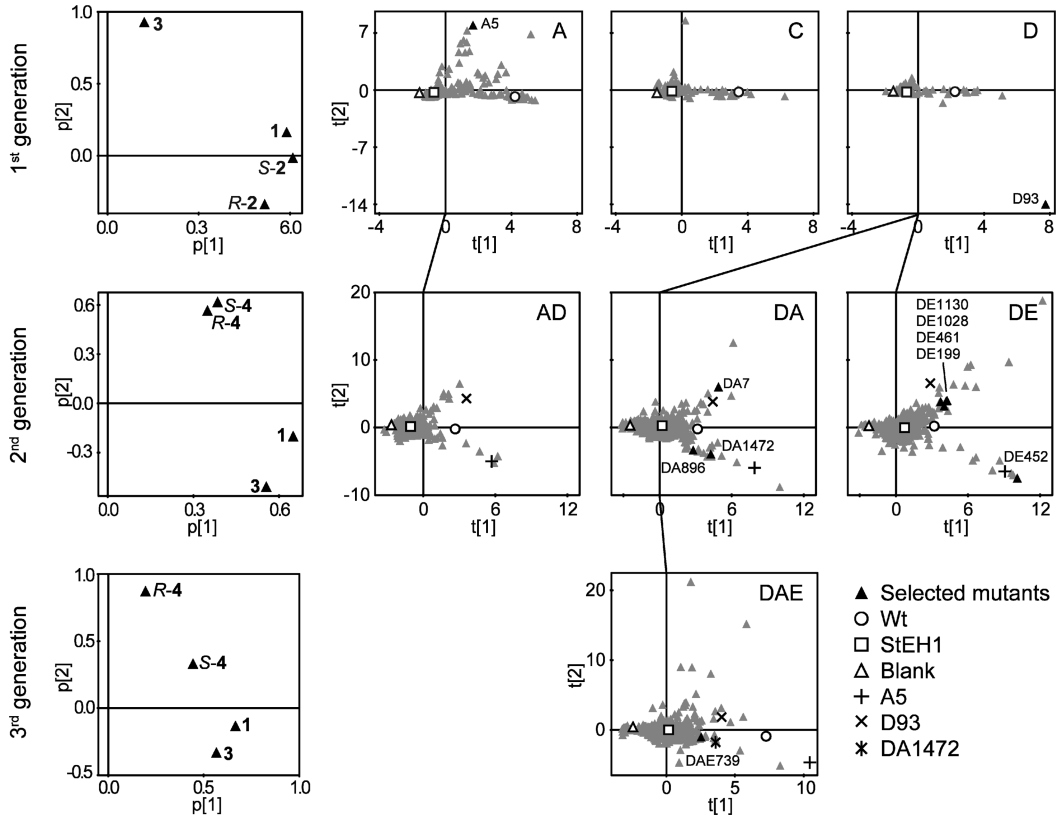

Figure 2. Principal component analysis on normalized library screening activities. The loading plots (left panel) describe the relationships between the screening substrates. Substrates are indicated by black triangles. The score plots (the three panels to the right) displays the observations projected from K-space into two dimensions. The analysis was performed on the total data set per generation of library (1st, 2nd, and 3rd). To aid in the interpretation of the score plots only one library is shown per plot. All library clones and a mean value of the controls are shown as a triangle. Symbols key is shown in the lower right corner. Library clones are in gray triangles and hits are in black triangles. Clones containing template genes were added as controls to 2nd and 3rd selection rounds, and their scores are shown by the respective symbols.

6.22 mM^{-1} cm^{-1}) in real time, using a Molecular Device SpectraMAX 190 plate reader. Oxidation of alcohol substrates were performed in 0.1 M glycine-NaOH, pH 10.0, and in the presence of 0.2 mM NAD^+. Reduction of aldehyde **3** was performed in 0.1 M sodium-phosphate, pH 7.0, and in the presence of 0.2 mM NADH. First-generation library clones were screened for enzymatic activity with, 6 mM 1-propanol (**1**), 2.5 mM *S*-propanediol (*S*-**2**), 40 mM *R*-propanediol (*R*-**2**), and 34 mM phenylacetaldehyde (**3**). In screening of second- and third-generation clones the propanediols were substituted by *S*- and *R*-3-phenylpropane-1,2-diol (*S*- and *R*-**4**), concentrations used were 5 mM **1**, 20 mM **3** and 10 mM of *S*- or *R*-**4**. The genes encoding selected hits were sequenced in full to identify introduced mutations and to exclude other alterations.

Larger Scale Expression and Purification of FucO Variants. C-terminally 5-His-tagged FucO mutants were expressed in 0.5 L cultures according to the protocol previously described.[12] After centrifugation the cells were frozen at −80 °C until purification. Frozen bacteria pellets were thawed and resuspended in binding buffer (20 mM imidazole, 0.5 M NaCl, 20 mM sodium-phosphate, pH 7.5 and 0.02% (w/v) NaN_3), up to a final volume of approximately 25 mL. Cells were lysed using a cell disruptor (Constant systems Ltd.), and the lysate was cleared by centrifugation at 38,000 *g* for 1 h at 4 °C. Cleared lysate was mixed with 1 mL of Chelating Sepharose Fast Flow resin charged with Ni^{2+} ions and incubated for 30 min at 4 °C. The slurry was subsequently centrifuged for 5 min at 800 *g*, and the supernatant was carefully discarded. Unspecifically bound proteins were eluted by resuspension of resin in 20 mL wash buffer (60 mM imidazole, 0.5 M NaCl, 20 mM sodium-phosphate, pH 7.5 and 0.02% (w/v) NaN_3), incubation for 10 min, centrifugation for 5 min at 800 *g* and discarding the supernatant. This wash step was repeated twice. Bound enzyme was eluted by addition of 2.5 mL elution buffer (300 mM imidazole, 0.5 M NaCl, 20 mM sodium-phosphate, pH 7.5, and 0.02% (w/v) NaN_3), incubation for 5 min followed by 7 min centrifugation at 800 *g*. The elution was repeated twice. The two elution fractions were desalted using a PD-10 column equilibrated with 0.1 M sodium-phosphate, pH 7.4, fortified with 0.02% (w/v) NaN_3. All purification steps were carried out at 4 °C and all incubations were performed on a rocking-table. Purity of protein variants were determined by SDS-PAGE stained with Coomassie Brilliant Blue R-250. Concentrations of purified proteins were determined from their absorbances at 280 nm using an extinction coefficient of 41 000 M^{-1} cm^{-1}.[12] All kinetic measurements were conducted within two weeks after purification

Kinetic Characterization of FucO Variant Enzymes. Catalyzed initial rates were measured, and the steady-state parameters k_{cat}, K_M, and k_{cat}/K_M were extracted essentially as described in ref 12, with the exception that each substrate concentration was measured in duplicates. Measurements with **3** were performed in a Molecular Device SpectraMAX 190 plate reader. Activities with *S*- and *R*-**4** were performed in a Shimadzu UV-1700 spectrophotometer.

dx.doi.org/10.1021/cs400824h | *ACS Catal.* 2013, 3, 3016−3025

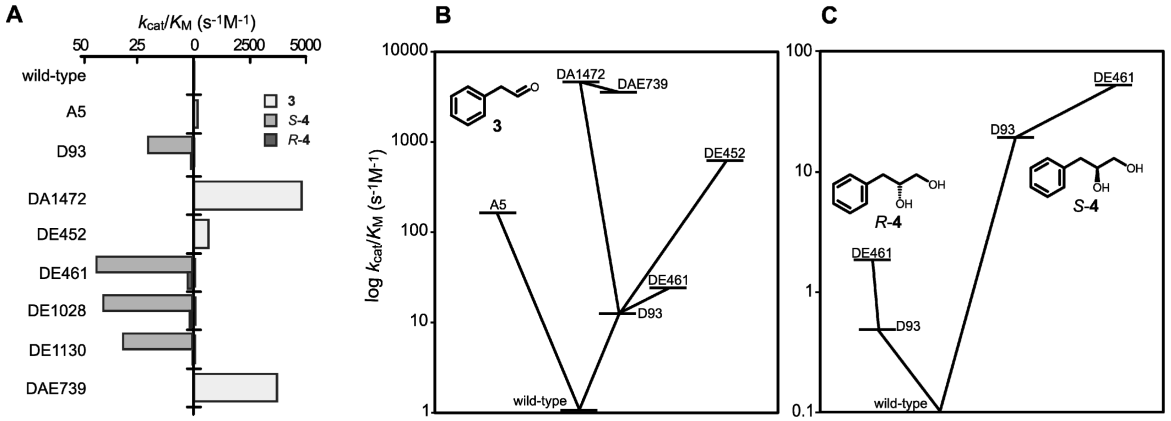

Figure 3. (A) Bar chart of catalytic efficiencies of FucO variants obtained from the directed evolution. Bars to the left show k_{cat}/K_M (s^{-1} M^{-1}) with the respective enantiomers of diol **4** and bars to the right with aldehyde **3**. (B and C) Evolutionary pathways for improvements in catalytic activity with **3** (B) or the different enantiomers of **4**.

Multivariat Data Analysis of Screening Data. Principal component analysis was performed on initial reaction velocities recorded during library screening using SIMCA-P+ 12.0.1 (Umetrics). Rows in the data matrix corresponded to the different screening substrates and columns corresponded to the reaction velocities displayed by the different clones. Clones displaying negative values were excluded from the data table. To not skew the analysis with data from control clones, mean values of these reaction velocities were used. Before analysis, the data was normalized to unit length and mean-centered. Three PCAs were performed, one for each library generation. For clarity, the data is graphically presented separately for each library. Figure 2 shows PC1 versus PC2 and display library distributions with controls and improved variants indicated.

Structural Modeling and Docking. The three-dimensional structures of FucO mutants DA1472 (N151G, L259V) and DE461 (V164C, L259V, C362G) were modeled based on the crystal structure of FucO in complex with NAD$^+$ (PDB code 2BL4[15]). A set of ten models with NAD$^+$ and Fe(II) in the active site was created with MODELLER,[22] and the model with the lowest value of the MODELLER objective function was used for docking studies. **3** was directly taken from the crystal structure of *E. coli* amine oxidase (PDB code 1D6U[23]) for ligand docking, while (2*R*, 3*S*)-3-amino-3-phenylpropane-1,2-diol was derived from the crystal structure of *Scytalidium lignicola* Scytalidopepsin B (PDB code 2IFR[24]) and edited to *S*-**4** with Maestro Molecular Modeling Interface (Version 9.3., Schrödinger, Inc.). All protein structures and the substrates were prepared for docking in Discovery Studio (Version 3.5, Accelrys Inc.), which was also used to detect receptor cavities and the active site cavities. In the active sites of the proteins, O7N was constrained as acceptor of hydrogen bonds, and H23/H25 of NAD$^+$ were defined as hydrogen bond donor and acceptor, respectively. In *S*-**4**, O1 and O5 were constrained as hydrogen bond acceptors, and H22 and H23 as donors, while O9 in **3** was a possible acceptor. GOLD via Discovery Studio (Version 3.5, Accelrys Inc.) was used to perform the docking of **3** to the DA1472 mutant, *S*-**4** to the DE461 mutant, and both substrates to the wild-type FucO. The docking poses were analyzed and scored with the Score Ligands function in Discovery Studio (Version 3.5, Accelrys Inc.), and the pose with the highest PLP2 score was chosen as the best pose. PyMOL (Version 1.5, Schrödinger, LLC) was used to prepare pictures of the complexes.

RESULTS

Enzyme Libraries Designed to Facilitate the Isolation of Functional FucO Variants. To streamline screening of variants, the gene libraries were in all cases constructed from limited codon subsets[25] (Table 1). To increase the chances of generating mutants capable of binding bulky substrates, mutagenesis in the first-generation libraries introduced mainly replacements of smaller amino acid residues in the lining of the entrance to the active site. In the subsequent second and third-generation libraries, codon sets allowing for insertion of also other residues were included to increase the repertoire of functional groups. The codon and mutation distributions of the different libraries were assayed by sequencing randomly picked sets of unselected library clones. Although minor skewing of the theoretical codon distribution was observed at some sites, the library qualities were considered to be adequate.

Isolation of Dehydrogenase Variants Exhibiting Activity with Aryl-Substituted Substrates. Although the aim was to isolate FucO variants that had achieved activity with the 3-phenyl-1,2-propanediols (**4**; Chart 1), phenylacetaldehyde **3** was used in the initial rounds as surrogate substrate. The motives for this choice were as follows. (i) The reduction reaction is thermodynamically favorable and proceeds with at least 1 order of magnitude faster rates as compared to the oxidation reaction;[12] hence, an increased sensitivity during screening, facilitating detection of also low-activity variants, was anticipated. (ii) **3** was judged to be a reasonable structure analogue of the aldehyde derivatives of **4**. It should be noted, however, that **3** does not contain a *sec*-alcohol at the α-position and lacks one methylene group. Therefore, any (critical) influence that this structural difference might cause was expected to impact the selection outcome.

In the first screening round, *S*- and *R*-1,2-propanediol (**2**) were included as screening substrates to probe the enantioselectivity of new dehydrogenase variants. During screening of second and third-generation libraries, the respective enantiomers of **4** replaced the propanediol substrates. 1-Propanol (**1**) was included in all screening rounds as a control substrate to assay the presence of (any) alcohol dehydrogenase activity.

Screening enzyme libraries for activity with several substrates rapidly generates a very large data set. To get an overview of the screening outcome, principal component analysis (PCA) was performed on normalized enzyme activities. The PCAs for the

dx.doi.org/10.1021/cs400824h | ACS Catal. 2013, 3, 3016−3025

different libraries are presented in Figure 2. The analysis provided a comprehensive view of the clone distributions in the respective libraries and was also consulted in scoring of possible hits. The 10−20 best variants from each library were rescreened, and their corresponding genes were sequenced to confirm their initial scoring as hits and to deduce their protein sequences.

FucO variant hits were expressed and purified by Ni(II)-IMAC and their activity profiles were determined using substrates **3** and *S*- and *R*-**4**. The selected clones are marked in the PCA (Figure 2). Enzymatic efficiencies for clones active with these substrates are graphically presented in Figure 3 and listed in Table 2, together with determined values of kinetic parameters. Activities for purified and characterized clones, which showed no elevated activity with the desired substrates, are not presented.

First-Generation Clones. The PCA of screening activities displayed that clones in the first generation were grouped into three distinct clusters (Figure 2). One cluster showed activities similar to the wild-type enzyme (circle in Figure 2). Another group displayed increased activity with **3**, but had lost activity with both enantiomers of **2**. Clones populating the third cluster displayed reasonable activity with **3** and had retained some activity with *S*- or *R*-**2**. Approximately 70% of the analyzed clones did not display activity above background rates with any of the screening substrates and were considered to represent inactive clones.

Library A. Eight of the FucO variants were selected for larger-scale expression, purification, and characterization. Of the characterized mutants, variant A5 (N151G) displayed the most interesting properties with a marked increase in the catalytic activity with aldehyde **3**; 90- and 150-fold increases in k_{cat} and k_{cat}/K_M, respectively. Although A5 displayed considerable activity with **3**, this variant did not catalyze the oxidation of the *S*- or *R*-**4** diols.

Library C. One clone was scored as a positive hit with aldehyde **3**. However, the purified enzyme did not show any noteworthy increase in activity with any of the aryl-substituted substrates.

Library D. Two clones were chosen for characterization; one displaying activity with **3** and one clone displaying a remarkably higher activity than the wild-type with *R*-**2**. The clone with **3**-activity turned out to have no increased activity with the aryl-substituted substrates. Nevertheless, variant D93 (L259V), selected because of its increased *R*-**2** activity, turned out to display reasonable activity also with the targeted diol **4**. D93 showed activity with *S*-**4** with a k_{cat} of 0.15 s^{-1} and a K_M of 6.6 mM. The k_{cat}/K_M value for the two different enantiomers were determined to be 20 s^{-1} M^{-1} for *S*-**4** and 0.5 s^{-1} M^{-1} for *R*-**4**, resulting in an E-value (*S*/*R*) of 40. This mutant also displayed a 10-fold increase in k_{cat}/K_M with **3** as compared to the wild-type, mainly due to a 30-fold increase in k_{cat}.

Second Generation Clones. Variant A5 (plus sign in Figure 2) was used as template in the construction of library AD and D93 (cross in Figure 2) for libraries DA and DE. PCA of clone activities displayed two clusters (Figure 2). As compared to the wild-type, one cluster had elevated activity with *S*- and/or *R*-**4**, similar to D93. The other cluster had elevated activity with aldehyde **3**, similar to the A5. All three libraries displayed similar patterns. Approximately 90% of the screened clones did not show activities with any of the screening substrates.

Table 2. Steady-State Kinetic Parameters of FucO Variants

enzyme variant	mutation	k_{cat} (s^{-1})	K_M (mM)	k_{cat}/K_M (s^{-1} M^{-1})
		Phenylacetaldehyde (**3**)		
wild type		0.023 ± 0.01	23 ± 10	1.1 ± 0.2
A5	N151G	2.1 ± 0.1	12 ± 0.7	170 ± 5
D93	L259V	0.62 ± 0.1	48 ± 12	13 ± 0.8
DA1472	N151G, L259V	21 ± 1	4.4 ± 0.7	4800 ± 500
DE199	V164I, L259V, C362A	n.s.[a]	n.s.	4.9 ± 0.3
DE452	*V153I*, V164I, L259V	4.0 ± 0.3	6.2 ± 1	640 ± 60
DE461	V164C, L259V, C362G	2.5 ± 0.4	100 ± 20	25 ± 1
DE1028	V164M, L259V, C362Y	1.4 ± 0.2	29 ± 8	48 ± 4
DE1130	V164I, L259V	0.90 ± 0.1	38 ± 6	24 ± 1
DAE739	N151G, V164I, L259V, C362N	21 ± 2	5.7 ± 1	3700 ± 400
		S-3-Phenylpropane-1,2-diol (*S*-**4**)		
wild type				n.d.[b]
A5	N151G			n.d.
D93	L259V	0.15 ± 0.004	6.6 ± 0.4	20 ± 1
DA1472	N151G, L259V			n.d.
DE199	V164I, L259V, C362A	0.20 ± 0.01	16 ± 2	12 ± 0.6
DE452	*V153I*, V164I, L259V			n.d.
DE461	V164C, L259V, C362G	0.32 ± 0.01	7.3 ± 0.4	43 ± 2
DE1028	V164M, L259V, C362Y	0.25 ± 0.005	6.3 ± 0.3	40 ± 1
DE1130	V164I, L259V	0.29 ± 0.01	9.3 ± 0.5	31 ± 1
DAE739	N151G, V164I, L259V, C362N			n.d.
		R-3-Phenylpropane-1,2-diol (*R*-**4**)		
wild type				n.d.
A5	N151G			n.d.
D93	L259V	n.s.	n.s.	0.50 ± 0.1
DA1472	N151G, L259V			n.d.
DE199	V164I, L259V, C362A	n.s.	n.s.	0.19 ± 0.03
DE452	*V153I*, V164I, L259V			n.d.
DE461	V164C, L259V, C362G	0.050 ± 0.005	26 ± 4	1.9 ± 0.1
DE1028	V164M, L259V, C362Y	0.010 ± 0.001	9.8 ± 2	1.0 ± 0.1
DE1130	V164I, L259V	0.014 ± 0.003	35 ± 11	0.40 ± 0.05
DAE739	N151G, V164I, L259V, C362N			n.d.

[a] n.s., Enzyme saturation was not reached within the practically useful substrate concentrations. Only k_{cat}/K_M could therefore be determined. [b] n.d., No enzyme activity detected.

Library AD. From the initial screen 10 clones were selected as potential hits. However, after rescreening none of these variants were selected for further characterization, because of their apparent low absolute activities.

Library DA. After rescreening and sequencing three variant enzymes were selected for purification and further characterization. Although the template D93 displays activity with both **4** diols, two of the three characterized enzymes had lost most of their diol oxidation activities but instead showed improved activity with aldehyde **3**, which lacks the α-hydroxyl group. The most efficient catalyst was DA1472 (N151G, L259V) with k_{cat} and K_M values for **3** of 21 s^{-1} and 4.4 mM, respectively. This is so far the most active variant with this substrate, and it

dx.doi.org/10.1021/cs400824h | ACS Catal. 2013, 3, 3016−3025

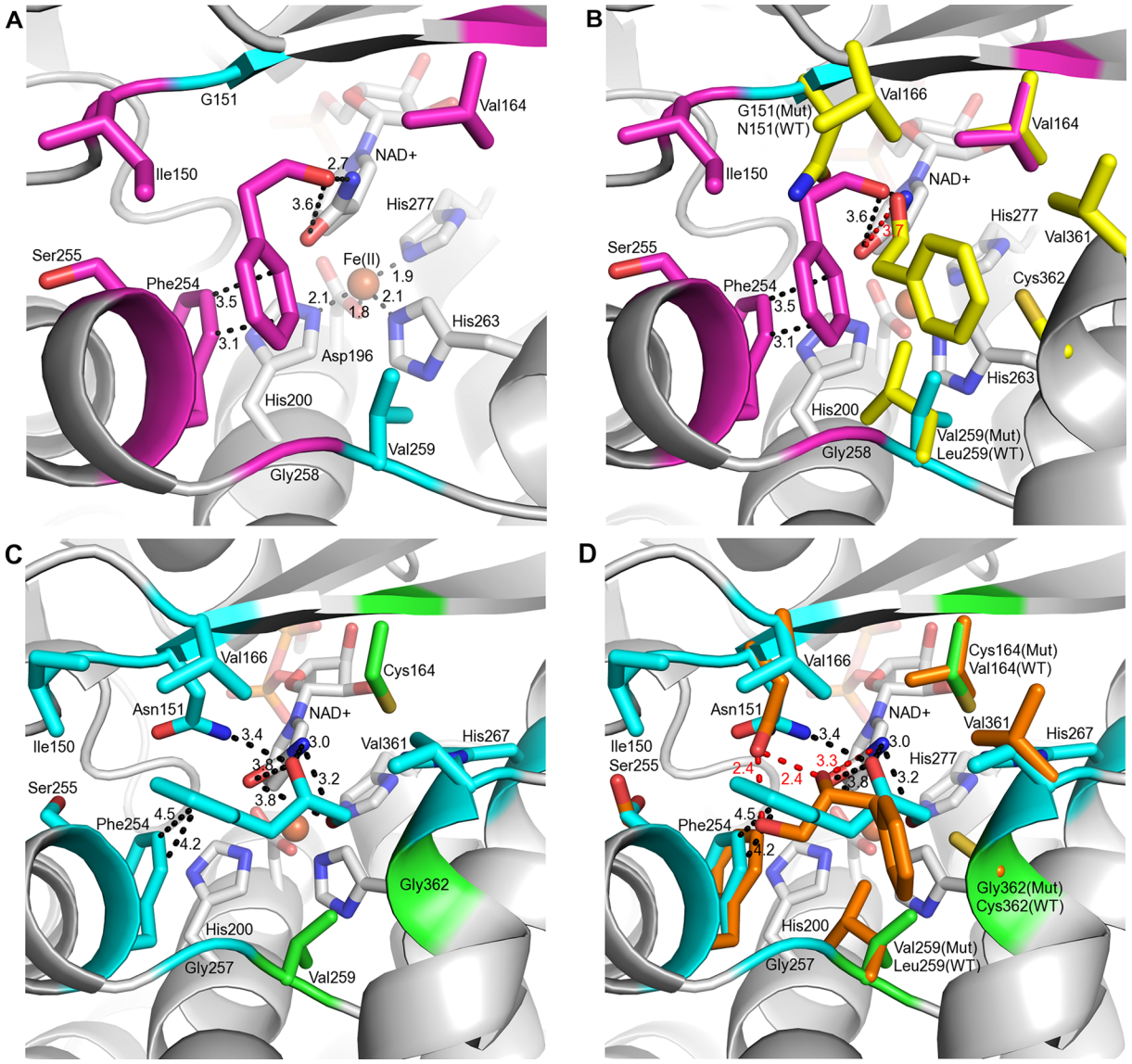

Figure 4. (A) **3** (pink) binds in a bent conformation to the DA1472 (N151G, L259V) mutant (cyan), which enables it to hydrogen bond to NAD^+ and $\pi-\pi$ stack with F254. Residues within 4 Å from **3** are shown as pink sticks. The iron-binding residues are shown as gray sticks. (B) In the wild-type protein, **3** binds in a more extended conformation (yellow) than in the mutant (pink). This makes it impossible for **3** to $\pi-\pi$ stack with F254 in the wild-type protein. Residues within 4 Å from **3** are shown as sticks in pink (mutant) and yellow (wild type). The mutations are marked in cyan. (C) *S*-**4** (cyan) binds in a bent conformation to the DE461 (V164C, L259V, C362G) mutant (green) and hydrogen bonds to NAD^+ and N151, while $\pi-\pi$ stacking with F254. Residues approximately 4 Å from *S*-**4** are shown as cyan sticks. (D) In the wild-type protein, *S*-**4** is docked in a more extended conformation (orange) than in the mutant (cyan). This makes it impossible for *S*-**4** to $\pi-\pi$ stack with F254 in the wild-type protein. Additionally, only one of the hydroxyl groups of *S*-**4** is able to hydrogen bond to NAD^+ in the wild-type complex, while *S*-**4** in the DE461 mutant hydrogen bonds via both hydroxyl groups. Residues approximately 4 Å from *S*-**4** are shown as sticks in cyan (mutant) and orange (wild type). The mutations are marked in green. Hydrogen bonds and $\pi-\pi$ interactions between the docked substrates and the enzymes are shown in black dashed lines for the mutant proteins and in red dashed lines for the wild-type.

displayed a substantial 4400-fold increase in k_{cat}/K_M as compared to the wild-type enzyme and a 30-fold increase as compared to the A5 mutant.

Library DE. Eight enzyme variants were chosen for further characterization. Out of these, five displayed activity with the desired substrates. In this library, the most efficient clones with *S*- and *R*-**4** (Table 2) were found. DE461 (V164C, L259V, C362G), DE1028 (V164M, L259V, C362Y), and DE1130 (V164I, L259V) all displayed k_{cat} values for the *S*-enantiomer of approximately 0.3 s^{-1} and k_{cat}/K_M in the range 30−40 s^{-1} M^{-1}, which corresponds to a doubling as compared to the D93 template. With respect to the *R*-enantiomer, variants DE461 and DE1028 displayed 4- and 2-fold higher k_{cat}/K_M, respectively, as compared to the D93 variant. DE1130 had retained the relatively low activity with *R*-**4**, resulting in an improved enantioselectivity of *S*-**4** (E = 80). In addition, DE452 (V153I, V164I, L259V) had no detectable activity with diols **4** but had gained activity with aldehyde **3** with a k_{cat}/K_M of 640 s^{-1} M^{-1}. The V153I mutation had not deliberately been included in the library but was an artifact during library construction.

Third Generation Clones, Library DAE. The DA1472 variant (N151G, L259V, star in Figure 2) was used to template this library. PCA of screening activities revealed hits displaying

dx.doi.org/10.1021/cs400824h | *ACS Catal.* 2013, 3, 3016−3025

activity with **3**, *S*-**4**, or *R*-**4** (Figure 2). However, after rescreening, only one enzyme variant DAE739 (N151G, V164I, L259V, C362N) was selected for further characterization. It displayed a catalytic profile similar to that of the parental enzyme, with a k_{cat} of 21 s^{-1} and a K_M of 5.7 mM for **3** and without detectable activity with *S*- and *R*-**4**.

Structural Modeling and Docking Studies of Mutants. The docking results show that the DA1472 (N151G, L259V) and DE461 (V164C, L259V, C362G) mutants can accommodate the aryl-containing compounds, which makes it possible for them to use these as substrates. In the DA1472 mutant, the aldehyde oxygen of **3** hydrogen bonds with the amide of NAD^+ (Figure 4A). Additionally, the phenyl ring of **3** interacts through $\pi-\pi$ stacking with the phenyl ring of F254. Docking of the same substrate to the wild-type protein indicates that, because of a different conformation of **3** in the wild-type active site, the $\pi-\pi$ stacking interaction between the phenyl ring and F254 is lost (Figure 4B). In the wild type, the substrate adopts an extended conformation with the phenyl ring protruding from the active site cavity, while the same substrate binds in a bent conformation to the DA1472 mutant. When the conformation of **3** in the mutant is compared to the wild-type structure, it becomes clear that N151 in the wild-type protein inflicts structural clashes, which prevents binding of this compound in the same conformation as in mutant DA1472 (Figure 4B). Similarly to the DA1472 mutant complex, *S*-**4** is docked to the DE461 mutant in a bent conformation, which enables the phenyl ring of the substrate to form $\pi-\pi$ stacking interactions with F254 (Figure 4C). Once again, this interaction is lost in the wild type-*S*-**4** complex, where the extended conformation of *S*-**4** causes the phenyl ring to point away from F254 (Figure 4D). In the DE461 mutant, the L259V mutation makes the active site cavity bigger, which enables *S*-**4** to bind in a bent conformation. In the wild-type enzyme, the extended conformation of *S*-**4** allows hydrogen bonding to N151 through both hydroxyl groups, while only the α-hydroxyl group is able to hydrogen bond to NAD^+ (Figure 4D). When *S*-**4** is docked to the DE461 mutant the α-hydroxyl group hydrogen bonds to N151, and both hydroxyl groups make a hydrogen bond to NAD^+. This is due to the C362G mutation, which creates more space for the ligand and enables *S*-**4** to bind in a different conformation to the DE461 mutant as compared to the wild-type enzyme (Figure 4D).

DISCUSSION

In today's world of increasing environmental pressure, there is a growing need for "greener" solutions within chemical manufacturing. During the past 10 years, the use of enzymes in industrial applications such as synthesis of fine chemicals,[26] pharmaceuticals,[27] bioenergy,[28] agriculture,[29] textile industry,[30] and degradation of pollutants[31] has increased.[10] Biocatalysts are being established as environmentally friendly alternatives to contemporary technologies since they are efficient also under mild reaction conditions: moderate temperatures, aqueous solutions, and usually without requirement for noble and other rare metals. Furthermore, enzymes are produced from renewable sources, are fully biodegradable and nontoxic. To utilize the catalytic efficiency of enzymes in useful applications, however, they must often undergo re-engineering to become customized for the reaction at hand.

In this study, we successfully modified a propanediol oxidoreductase, specialized by nature to catalyze the oxidation/reduction of low-molecular 1,2-diols/α-hydroxy aldehydes, into variant enzymes capable of catalyzing the oxidation and reduction of also bulkier substrates. From only two rounds of (semi)saturation mutagenesis of noncatalytic active-site residues, we succeeded to generate enzyme variants that catalyze the oxidation of 3-phenyl-1,2-propanediol (**4**), a substrate with which the wild-type FucO shows no detectable activity. All these variants displayed retained enantiopreferences favoring the *S*-enantiomer although *R*-**4** was also accepted as substrate to different degrees. The most stereoselective variant DE1130, displays an E-value of 80 preferring the *S*-enantiomer of **4** and can thus be classified as adequately selective for synthetic purposes.[32] Enzyme variants with increased activity with phenylacetaldehyde (**3**) were also obtained, with the second-generation mutant DA1472 exhibiting a 4400-fold increased catalytic efficiency as compared to the wild-type. The turnover number displayed by this mutant approaches the highest k_{cat} values so far measured for FucO with any aldehyde.[12]

The choice of FucO as starting scaffold for the engineering was based on the following criteria. (i) The enzyme catalyzes the oxidation of the primary alcohol carbon of vicinal diols with high (absolute) regioselectivity. This is a rare feature in alcohol dehydrogenases and is, besides FucO, found only in certain carbohydrate dehydrogenases such as glycerol dehydrogenase. (ii) The enzyme is readily produced in an expression system allowing for directed evolution. (iii) The enzyme structure, both tertiary and oligomeric, is comparably simple which further facilitates enzyme purification, characterization, and manipulation. In comparison to the glycerol dehydrogenases, which are octameric proteins,[33,34] FucO is a homodimer and a native *E. coli* enzyme.

The screening method used (detection of NADH absorbance) is simple and sensitive enough to make it possible to search for activities with different substrates in parallel. Since library screening often represents a bottleneck in directed evolution, this simplicity and sensitivity of the screen is of great advantage. The use of principal component analysis also helped to achieve an overview and to visualize the activity distributions within the different mutant-libraries. This allowed us to explore multiple simultaneous evolutionary pathways in parallel (Figure 3B, C).

FucO-catalyzed rates of aldehyde reductions are at least 1 order of magnitude faster than alcohol oxidations. Hence, to increase the sensitivity of the screen and still select for variants with low but improved activity with aryl-substituted substrates, **3** was used as a surrogate substrate in the search for enzymes active with diols **4**. It has been shown in a related study of in vitro evolution of steroid hormone receptors, that coevolution of highly specialized proteins can be successfully accomplished by iteratively selecting for activity toward structural intermediates of the ultimate target ligand.[35] Our results show that **3** was not an optimal intermediate, since variants active with one substrate were often not active with the other. It can be speculated whether these differences depend on the absence of the secondary alcohol group in **3** or the fact that the distance between the redox-active carbon and the phenyl substituent is shorter in **3** as compared to **4**. Nevertheless, the results demonstrate that the FucO enzyme has the inherent ability to be modulated to catalyze reactions with different types of substrates.

Unveiling Silent Enzyme Activities. The FucO enzyme can be viewed as evolutionary very well adapted for catalyzing the reduction of *S*-lactaldehyde into *S*-1,2-propanediol. The

dx.doi.org/10.1021/cs400824h | ACS Catal. 2013, 3, 3016−3025

reaction plays an important role in the anaerobic catabolism of L-fucose since the reaction replenishes the NAD^+ pool and the product diol is readily excreted as a terminal fermentation product.[36] No other metabolic role has been assigned to this enzyme, and its structure/activity profile, which describes high selectivity for the *S*-enantiomer of small aliphatic alcohol/aldehyde substrates, further supports its assigned role in intermediary metabolism.[12,15] The evolvability of such specialized enzymes has been questioned and "generalist" enzymes with broad substrate scope are considered to be more malleable (cf. ref 37). The outcome from the present work is partly in agreement with this view since relatively few amino acid residue replacements were apparently allowed at the chosen sites of mutagenesis to generate functional variants (Figure 3B, C). On the other hand, our results in the directed evolution of FucO certainly also support the notion that the evolvability of enzyme function relies on underlying, undisclosed promiscuous activities that may be observed upon limited structural changes, that is, by few mutation events.[38] The structural difference caused by the single mutation in variant D93 (L259V) corresponds to only one methylene bridge less. This minor modification still unveils the (hidden) potential of this enzyme to catalyze the conversion of the bulky *S*-**4** diol into the *S*-α-hydroxy aldehyde. To give a measure of the magnitude of improvement in catalytic activity with this substrate is problematic since the wild-type enzyme does not accept this substrate at all (from an estimated level of detection of *any* catalytic activity one may assume a more than 1000-fold improvement in catalytic activity from the L259V mutation). Introducing a smaller steric constraint (more volume) at an appropriate position was in this case enough to expose this new catalytic activity of FucO.

Creating additional volume in the active site is not the only solution to achieve catalytic activity with *S*-**4**. This is demonstrated by mutagenesis at the E-site (V164 and C362 in Figure 1C). In this case, several of the mutations introduced bulkier amino acid residues; variant DE1028 (V164M, L259V, C362Y), DE461 (V164C, L259V, C362G), and DE1130 (V164I, L259V) all display twice as high activity as the template L259V with this substrate. It is also noteworthy that throughout the evolution process, F254, was retained in all variants displaying improved catalytic activity with the aryl-substituted substrates implying a role for its aromatic benzyl side-chain, as also suggested from the modeling.

The mutation of asparagine to glycine at position 151 is an even clearer example of how activity with bulkier substrates can be disclosed by simply removing sterical hindrance in the entrance to the active site. This mutation recurs in all variants (except DE452) which display activity with **3**. The cause, as deduced from the docking, is that F254 stabilizes the interactions between the substrates and the mutant proteins, thereby facilitates catalysis. Hence, it is possible that the hydrogen bonding capacity of **3** and *S*-**4** are insufficient to form adequately stable and productive enzyme−substrate complexes. The removal of the sterical hindrance resulting from the N151G mutation enables a stable binding of **3** which may contribute to the observed improvement in the catalytic efficiency with this substrate. The further improved activity resulting from the additional L259V mutation might be because the substrate aryl ring can come even closer to F254 and further stabilize productive substrate−protein interactions. Since the activity of DE739 (N151G, V164I, L259V, C362N) is similar to that of the DAE1472 variant, the mutations at positions 164 and 362 do not seem to affect the activity to any appreciable level.

The introduction of the N151G mutation renders the FucO variants nearly inactive with diol **4**. This may be because hydrogen bonding interactions between the α-hydroxyl of *S*-**4** and the N151 side-chain amide are lost (Figure 4C). The observation that clones active with **4** are inactive with **3** and vice versa is displayed also in the screening result (Figure 2), where the library distribution in generation two and three are divided into two quite distinct clusters, one displaying activity with **4** and one with **3**.

In variant DE452 an unexpected mutation, V153I, was introduced. Mutagenesis at this site was not designed for but became incorporated through imperfect PCR. Position 153 is situated further into the active site tunnel, in the second sphere from the residues included in the constructed libraries. DE452 and DE1130 only differ by this point-mutation. The resulting structural change is minor, with one γ-methyl group introduced in DE452. The activity profile, however, is drastically shifted: DE1130 is active with both enantiomers of **4** but displays comparably poor activity with aldehyde **3**. DE452, in contrast, is inactive with diols **4** but is highly active with **3**. Apparently, the additional methyl group in I153 prevents productive binding of the phenylpropanediols but favors binding of aldehyde **3** by 8.3 kJ/mol (as calculated from the respective k_{cat}/K_M values of DE452 and DE1130). These results also demonstrate that there is room for further tailoring of the substrate selectivity and that positions other than those visited in this study should be included.

CONCLUSION

The employment of enzymes in chemical synthesis requires the availability of biocatalysts with the adequate functional and physicochemical properties. We have in this work demonstrated the feasibility of evolving the substrate scope of a specialist enzyme, *E. coli* propanediol oxidoreductase FucO, to also accept bulky aryl-substituted substrates. The evolution process has revealed that few, often conservative but critically positioned, substitutions are enough to achieve large improvements in catalytic activities (Figure 3). The modeling and docking results present a possibility that the larger active site cavities in the mutant enzymes compared to the cavity in the wild type enzyme causes a gain in the important stabilizing interactions, which cannot be found in the complexes between the wild-type protein and studied substrates. On the contrary, the smaller active site cavity in the wild-type enzyme makes it impossible for it to use the studied bulky aryl-substituted molecules as substrates. The inherent enantioselectivity of the wild-type enzyme was retained in some evolved variants also when catalyzing the oxidation of the 3-phenyl-substituted derivatives of the native substrate 1,2-propanediol. We now have access to FucO variants that allows for the direct synthesis of the chiral α-hydroxy aldehydes *R*- and *S*-**5** as shown in Scheme 1B from a racemic mixture of an elemental starting material such as (2,3-epoxypropyl)benzene.

ASSOCIATED CONTENT

Supporting Information

Sequences of oligonucleotide primers are presented in Table SI1. This material is available free of charge via the Internet at http://pubs.acs.org.

AUTHOR INFORMATION

Corresponding Author

*E-mail: mikael.widersten@kemi.uu.se. Phone: +46 18 471 4992.

Notes

The authors declare no competing financial interest.

ACKNOWLEDGMENTS

The work of Hilde-Marlene Bergman is acknowledged. Prof. M. Johnson and Biocenter Finland (bioinformatics, structural biology, and translational activities) are acknowledged for the excellent computational infrastructure at the Structural Bioinformatics Laboratory, Åbo Akademi University and the National Doctoral Programme in Informational and Structural Biology is also acknowledged. This work was funded by the Swedish Research Council (MW, Grant #621-2011-6055), Sigrid Juselius Foundation (T.A.S., K.M.D.), Tor, Joe and Pentti Borg Foundation (T.A.S., K.M.D.), and Åbo Akademi Graduate School (K.M.D.).

REFERENCES

(1) Adams, R.; Levine, I. *J. Am. Chem. Soc.* **1923**, *45*, 2373−2377.
(2) Enders, D.; Bhushan, V. *Tetrahedron Lett.* **1988**, *29*, 2437−2440.
(3) Kratzer, R.; Nidetzky, B. *Chem. Commun.* **2007**, 1047−1049.
(4) Hoyos, P.; Sinisterra, J.-V.; Molinari, F.; Alcántara, A. R.; De María, P. D. *Acc. Chem. Res.* **2009**, *43*, 288−299.
(5) Lynch, J. E.; Eliel, E. L. *J. Am. Chem. Soc.* **1984**, *106*, 2943−2948.
(6) Goldberg, K.; Schroer, K.; Lütz, S.; Liese, A. 2007, *76*, 237−248.
(7) Blank, L. M.; Ebert, B. E.; Buehler, K.; Buhler, B. *Antioxid. Redox Signaling* **2010**, *13*, 350−393.
(8) Hall, M.; Bommarius, A. S. *Chem. Rev.* **2011**, *111*, 4088−4110.
(9) Monti, D.; Ottolina, G.; Carrea, G.; Riva, S. *Chem. Rev.* **2011**, *111*, 4111−4140.
(10) Bornscheuer, U. T.; Huisman, G. W.; Kazlauskas, R. J.; Lutz, S.; Moore, J. C.; Robins, K. *Nature* **2012**, *485*, 187−194.
(11) Cocks, G. T.; Aguilar, T.; Lin, E. C. *J. Bacteriol.* **1974**, *118*, 83−88.
(12) Blikstad, C.; Widersten, M. *J. Mol. Catal. B: Enzym.* **2010**, *66*, 148−155.
(13) Gurell, A.; Widersten, M. *ChemBioChem* **2010**, *11*, 1422−1429.
(14) Janfalk Carlsson, Å.; Bauer, P.; Ma, H.; Widersten, M. *Biochemistry* **2012**, *51*, 7627−7637.
(15) Montella, C.; Bellsolell, L.; Pérez-Luque, R.; Badía, J.; Baldoma, L.; Coll, M.; Aguilar, J. *J. Bacteriol.* **2005**, *187*, 4957−4966.
(16) Reid, M. F.; Fewson, C. A. *Crit. Rev. Microbiol.* **1994**, *20*, 13−56.
(17) Reetz, M. T.; Carballeira, J. D.; Vogel, A. *Angew. Chem., Int. Ed.* **2006**, *45*, 7745−7751.
(18) Reetz, M. T.; Prasad, S.; Carballeira, J. D.; Gumulya, Y.; Bocola, M. *J. Am. Chem. Soc.* **2010**, *132*, 9144−9152.
(19) Tang, L.; Gao, H.; Zhu, X.; Wang, X.; Zhou, M.; Jiang, R. *Biotechniques* **2012**, *52*, 149−156.
(20) Elfström, L. T.; Widersten, M. *Biochem. J.* **2005**, *390*, 633−640.
(21) Kille, S.; Acevedo-Rocha, C. G.; Parra, L. P.; Zhang, Z. G.; Opperman, D. J.; Reetz, M. T.; Acevedo, J. P. *ACS Synth. Biol.* **2013**, *2*, 83−92.
(22) Sali, A.; Blundell, T. L. *J. Mol. Biol.* **1993**, *234*, 779−815.
(23) Wilmot, C. M.; Hajdu, J.; McPherson, M. J.; Knowles, P. F.; Phillips, S. E. *Science* **1999**, *286*, 1724−1728.
(24) Pillai, B.; Cherney, M. M.; Hiraga, K.; Takada, K.; Oda, K.; James, M. N. *J. Mol. Biol.* **2007**, *365*, 343−361.
(25) Reetz, M. T.; Kahakeaw, D.; Lohmer, R. *ChemBioChem* **2008**, *9*, 1797−1804.
(26) Agudo, R.; Roiban, G.; Reetz, M. T. *ChemBioChem.* **2012**, *13*, 1465−1473.
(27) Savile, C. K.; Janey, J. M.; Mundorff, E. C.; Moore, J. C.; Tam, S.; Jarvis, W. R.; Colbeck, J. C.; Krebber, A.; Fleitz, F. J.; Brands, J.; Devine, P. N.; Huisman, G. W.; Hughes, G. J. *Science* **2010**, *329*, 305−308.
(28) Liu, X.; Bastian, S.; Snow, C. D.; Brustad, E. M.; Saleski, T. E.; Xu, J.; Meinhold, P.; Arnold, F. H. *J. Biotechnol.* **2012**, *164*, 188−195.
(29) Oliveira, G. R.; Silva, M. C.; Lucena, W. A.; Nakasu, E. Y.; Firmino, A. A.; Beneventi, M. A.; Souza, D. S.; Gomes, J. E., Jr; de Souza, J. D., Jr; Rigden, D. J.; Ramos, H. B.; Soccol, C. R.; Grossi-de-Sa, M. F. *BMC Biotechnol.* **2011**, *11*, 85.
(30) Cherry, J. R.; Lamsa, M. H.; Schneider, P.; Vind, J.; Svendsen, A.; Jones, A.; Pedersen, A. H. *Nat. Biotechnol.* **1999**, *17*, 379−384.
(31) van Leeuwen, J. G.; Wijma, H. J.; Floor, R. J.; van der Laan, J. M.; Janssen, D. B. *ChemBioChem* **2012**, *13*, 137−148.
(32) Bartsch, S.; Kourist, R.; Bornscheuer, U. T. *Angew. Chem., Int. Ed.* **2008**, *47*, 1508−1511.
(33) Ruzheinikov, S. N.; Burke, J.; Sedelnikova, S.; Baker, P. J.; Taylor, R.; Bullough, P. A.; Muir, N. M.; Gore, M. G.; Rice, D. W. *Structure* **2001**, *9*, 789−802.
(34) Lesley, S. A.; Kuhn, P.; Godzik, A.; Deacon, A. M.; Mathews, I.; Kreusch, A.; Spraggon, G.; Klock, H. E.; McMullan, D.; Shin, T.; Vincent, J.; Robb, A.; Brinen, L. S.; Miller, M. D.; McPhillips, T. M.; Miller, M. A.; Scheibe, D.; Canaves, J. M.; Guda, C.; Jaroszewski, L.; Selby, T. L.; Elsliger, M. A.; Wooley, J.; Taylor, S. S.; Hodgson, K. O.; Wilson, I. A.; Schultz, P. G.; Stevens, R. C. *Proc. Natl. Acad. Sci. U.S.A.* **2002**, *99*, 11664−11669.
(35) Chen, Z.; Zhao, H. *J. Mol. Biol.* **2005**, *348*, 1273−1282.
(36) Zhu, Y.; Lin, E. C. C. *J. Bacteriol.* **1989**, *171*, 862−867.
(37) Tracewell, C. A.; Arnold, F. H. *Curr. Opin. Chem. Biol.* **2009**, *13*, 3−9.
(38) Khersonsky, O.; Roodveldt, C.; Tawfik, D. S. *Curr. Opin. Chem. Biol.* **2006**, *10*, 498−508.